INTERNATIONAL JOURNAL OF PRECISION ENGINEERING AND MANUFACTURING Vol. 16, No. 1, pp. 31-41 JANUARY 2015 / 31
DOI: 10.1007/s12541-015-0004-6

Hysteresis Modeling of Magneto-Rheological Damper using Self-Tuning Lyapunov-based Fuzzy Approach

Dao Thanh Liem[1], Dinh Quang Truong[2], and Kyoung Kwan Ahn[2,#]

1 Graduate School of Mechanical Engineering, University of Ulsan, Daehakro 93, Namgu, Ulsan, South Korea, 680-749
2 School of Mechanical Engineering, University of Ulsan, Daehakro 93, Namgu, Ulsan, South Korea, 680-749
Corresponding Author / E-mail: kkahn@ulsan.ac.kr, TEL: +82-52-259-2282, FAX: +82-52-259-1680

KEYWORDS: Magneto-rheological fluid damper, Modeling, Online tuning technique

Magneto-rheological (MR) fluid damper is a semi-active control device that has recently received more attention because they offer the adaptability of active control devices without requiring the associated large power sources. But inherent nonlinear nature of the MR fluid damper is one of the challenging aspects for utilizing this device to achieve the high performance. So development of an accurate MR fluid damper model is necessary to take the advantages from its unique characteristics. The focus of this paper is to develop an alternative method for modeling a MR fluid damper by using a so-called self-tuning Lyapunov-based fuzzy model (STLFM). Here, the model is constructed in the form of a center average fuzzy interference system, of which the fuzzy rules are designed based on the Lyapunov stability condition. In addition, in order to optimize the STLFM, the back propagation learning rules are used to adjust the fuzzy weighting net. Firstly, experimental data of a damping system using this damper is used to optimize the model. Next, the optimized model is used to estimate online the damping performance in the real-time conditions. The modeling results prove convincingly that the developed model could represent satisfactorily the behavior of the MR fluid damper.

Manuscript received: July 17, 2014 / Revised: October 5, 2014 / Accepted: October 7, 2014

NOMENCLATURE

$V(\underline{x})$ = Lyapunov function candidate
f_{MR_est} = estimated damping force, *N*
f_{MR} = real damping force, N
in_1 = damper supplied current, *A*
in_2= damper rod displacement, *mm*
in_3 = damper velocity, *cm/s*
u_{LFI} = output of Lyapunov-Based Fuzzy Inference
k_{GFI} = output of Gain Fuzzy Inference
E = error function
N = number of triangle membership functions
a_j = center of j^{th} triangle of membership function
b_j = width of j^{th} triangle of membership function
$\mu_j(w_q)$ = height of the control GFI output
$w_j(w_q)$ = weight of the control GFI output
w_k = weight of LFI output
$\mu(w_k)$= height of LFI output
$\mu_{ij}(w_k)$ = consequent fuzzy output function
δ_{ij} = activating factor
η_a, η_a and η_c = learning rates

1. Introduction

In vibration field, vibration control techniques have classically been categorized into two areas, passive and active controls. Another semi-active control approach has been investigated by several researchers where it has better performance than passive control and required less power than active control.[1-9]

Among semi-active vibration control solutions, MR fluid dampers have recently received more attention. It is capable of generating a force with magnitude sufficient for rapid response in large-scale applications,[4-9] while requiring only a battery for power.[9] Additionally, these devices offer highly reliable operations and their performance is relatively insensitive to temperature fluctuations or impurities in the fluid.[10]

However, a major drawback that hinders its application rests with

the nonlinear force-displacement and hysteretic force-velocity characteristics. Therefore, one of the challenges involved in creating high performance MR fluid damper in control applications is the development of accurate models that can take full advantage of the unique features of the MR device. Both parametric and nonparametric models have been built by researchers to describe the behavior of MR fluid dampers.

There are several MR damper models proposed by researcher using a range of techniques. Models obtained by parametric approaches are known as Bingham, Bouc-Wen, phenomenological model and others.[11-14] The Bingham model[15,16] represents the dry-friction as a signum function on the damper velocity and may be considered as a simple model for describing the hysteresis characteristic. The Bouc-Wen model[16-21] uses a differential equation to depict the non-linear hysteresis with moderate complexity and is widely applied in building controls. The validity of these models for predicting the hysteresis behavior has been favorably proved by comparing with experimental results. One of the major problems in the Bouc-Wen model is the accurate determination of its characteristic parameters which is obtained by using optimization or trial-and-error techniques. In another study, Spencer et al[22] successfully developed a phenomenological model to improve the model accuracy with an additional internal dynamical variable. Chao and Lee[12] designed a hysteresis damper model based on a polynomial and a curve fitting to predict better the damping force when compared with conventional models. Although these parametric modeling methods could bring some favorable results, they required assumptions as regards the structure of the mechanical model that simulates behavior. The approach could be divergent if the initial assumptions for the model structure are flawed, or if the proper constraints are not applied to the parameters. Unrealistic parameters such as negative mass or stiffness may be obtained. Moreover, these techniques demanded high computational cost to generate and optimize the model parameters.

The nonparametric approaches to construct MR damper models were also developed by other researchers. Chang and Roschke[23] proposed a non-parametric model using multilayer perceptron neural network with optimization method for a satisfactory representation of a damper behavior. Schurter and Roschke[24] investigated the modeling of MR fluid dampers with an adaptive neural-fuzzy inference system. The fuzzy structure was simple for modeling; nevertheless, the training model process relied on input and output information on MR fluid dampers and took much computation time. Wang and Liao[14,25] explored the modeling of MR fluid dampers by using a trained direct identification based on recurrent neural network. Although, the designed models could predict the dynamic responses of the dampers with high precision, the model architectures and the training methods were complex.

For these reasons, a novel direct modeling method to model simply MR fluid dampers is proposed in this paper. This method uses a so-called self-tuning Lyapunov-based fuzzy model (STLFM) that is designed to overcome the disadvantages of conventional models. Here, the model is built in the form of a center average fuzzy interference system, of which the fuzzy rules are designed based on the Lyapunov stability condition to estimate directly the MR damping force output with respect to the MR characteristics. In addition, the back propagation learning rules are used to adjust the fuzzy weighting net to optimize the STLFM. A damping system using this damper was setup to investigate the design model. Experiments on this system are firstly conducted to acquire the data to optimize the model. Next, the optimized model is used to estimate online the damping performance in the real-time conditions. Effectiveness of the proposed modeling method is clearly verified through a comparison with the experimental data obtained from the test rig. The results show that the proposed fuzzy interference system designed by Lyapunov and trained online by neural technique has satisfactorily representative ability for the behavior of MR fluid damper with small computational requirement.

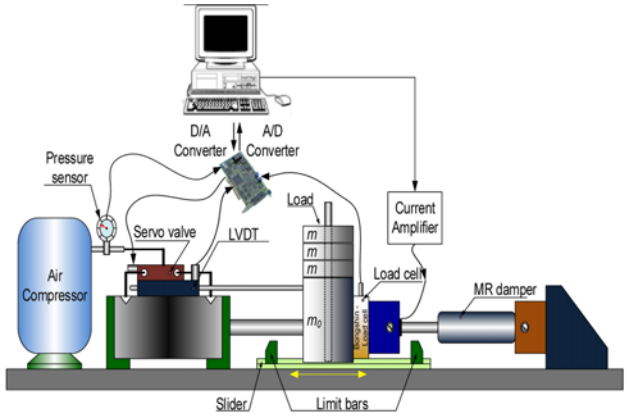

(a) Test setup Schematic for MR damper Identification

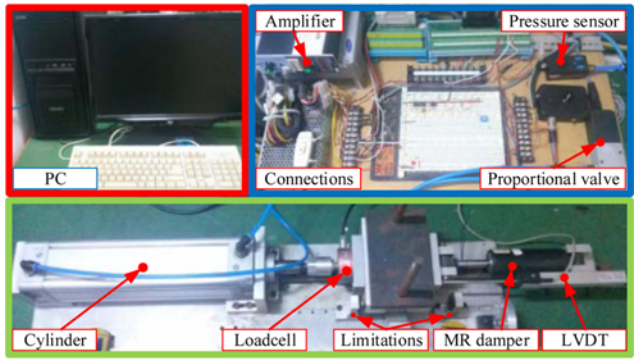

(b) Photograph of Test setup

Fig. 1 MR damper test Apparatus

2. Modeling of the MR Fluid Damper with the STF

2.1 Experimental apparatus

To evaluate the performance of MR dampers in vibration control application as well as to take a full advantage of the unique feature of these devices, a model is needed to accurately describe the behavior of the MR damper. The load frame shown in Fig. 1 was designed and built for the purpose of obtaining the MR damper response data necessary for identification studies. In this apparatus, the actuator end-effector is a pneumatic cylinder with 63mm diameter which is driven by a 5/3-way proportional valve manufactured by Festo Corp. to generate the vibration for the damping system. The spool motion of this servo valve is proportional to its control signal sent from a personal computer (PC)

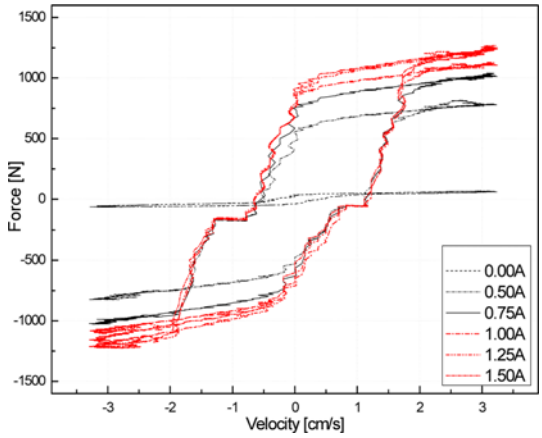

Fig. 2 Performance of MR damper with respect to a sinusoidal excitation at 1 Hz and 5 mm

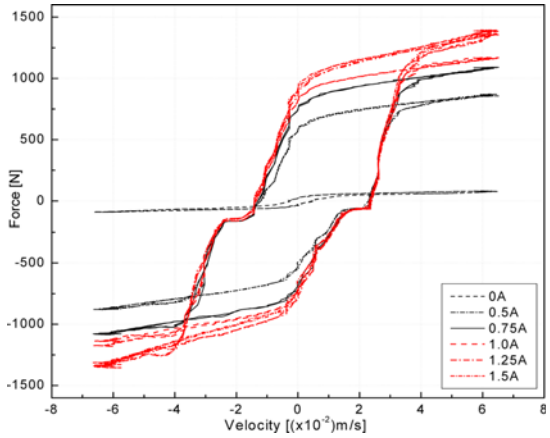

Fig. 4 Performance of MR damper with respect to a sinusoidal excitation at 2 Hz and 5 mm

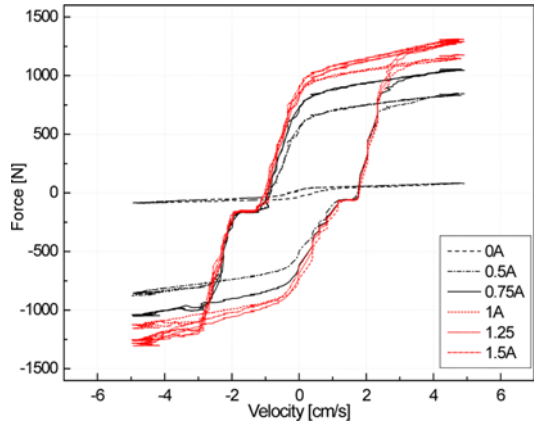

Fig. 3 Performance of MR damper with respect to a sinusoidal excitation at 1.5 Hz and 5 mm

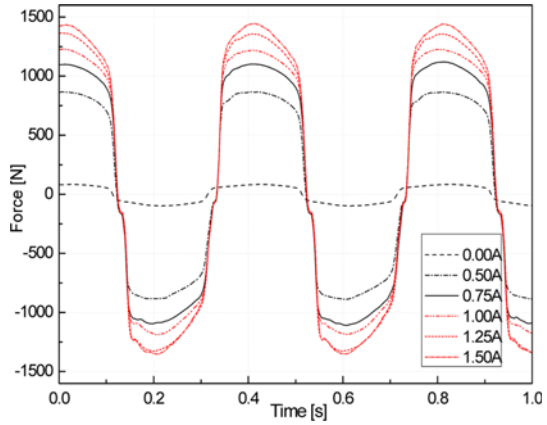

Fig. 5 Damping force vs. Time at sinusoidal excitation 2.5 Hz - 5 mm and (0-1.5) A

through a D/A converter of an Advantech multi-function card, PCI1711. A linear transducer (Novotechnik TR100) was fixed on the test rig base so that its slider contacts with the cylinder end-position to feed back the vibration information (as well as the damper rod displacement) to the PC. A Festo pressure sensor was attached to the system to manage the system pressure, and a ±500 Kg Bongshin load cell with the proper amplifier was attached in series with the damper to measure the actual damping force in order to compare with the force estimated by the models. For safety when doing experiments on the test rig, two limit bars were positioned at two sides of the loading system to restrict the piston movement and consequently, protect the load cell and MR fluid damper from damages.

2.2 Experiments on the test rig and data analysis

To obtain the data used to characterize the RD-1005-3 MR fluid damper behavior, a series of experiments on the rig was conducted under various sinusoidal displacement excitations while simultaneously altering the magnetic coil in a varying current range. The output of each test was the force generated by the damper (including all other factors such as friction forces) as shown in figures from 2 to 4.

Figures from 5 to 7 show an analysis of measurement results in

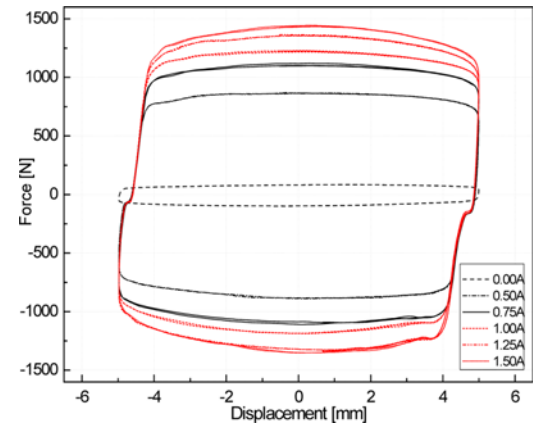

Fig. 6 Damping force vs. Displacement at sinusoidal excitation 2.5 Hz - 5 mm and (0-1.5) A

plots of force-time, force-displacement, and force-velocity relations with respect to a 2.5Hz sinusoidal excitation and 5mm of amplitude while the current supplied to the damper was in range between 0 and 1.5A. These relations point out that the damping force of the MR fluid

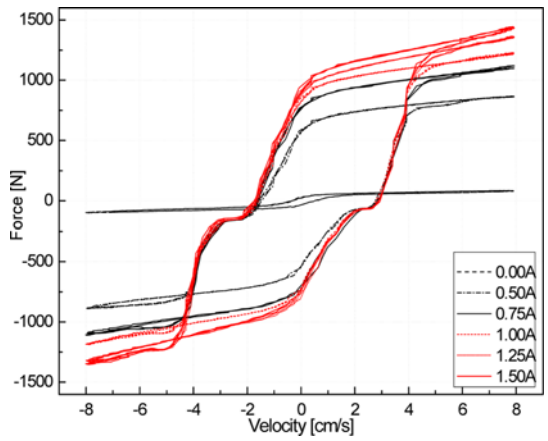

Fig. 7 Damping force vs. Velocity at sinusoidal excitation 2.5 Hz - 5 mm and (0-1.5) A

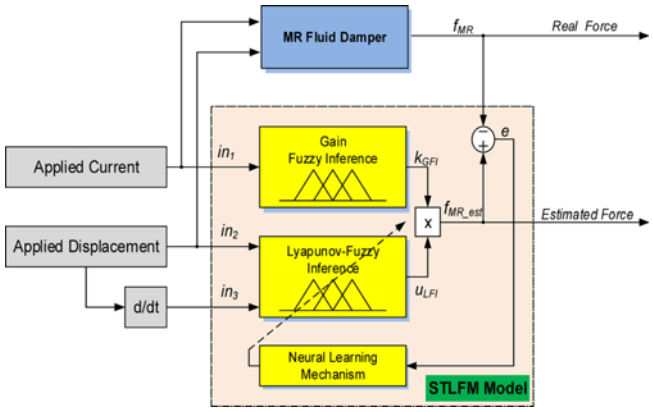

Fig. 8 Structure of the STLFM model

damper depends on the displacement/velocity of the damper rod and the current supplied for the damper coil.

2.3 Self-tuning Lyapunov-based fuzzy model for the MR damper

In this section, the design procedure of the proposed self-tuning Lyapunov-based fuzzy model (STLFM) is introduced. This model is based on center-average defuzzification architecture, which is a computationally efficient and well suited for implementation of nonlinear system. The most difficult aspect in designing a fuzzy controller is the construction of the rule base and membership functions (MFs).

It is known that neural network is capable to approximate any continuous function while Lyapunov theory is suitable for robustly designs of controllers and models. Hence in this paper, the back propagation algorithm with the gradient descent method is used to decide the shapes of MFs. Meanwhile, the Lyapunov synthesis method[26-28] is used to design the fuzzy inference. The fuzzy inference system then has higher learning ability that improves the control qualities. The overall structure of the STLFM model is shown in Fig. 8.

From this figure, it can be seen that the STLFM model consists of three main blocks which are: 'Gain Fuzzy Inference' (GFI) estimate the amplitude of damping force, 'Lyapunov-Based Fuzzy Inference' (LFI) to estimate the tendency of damping force, and 'Neural-Based Learning

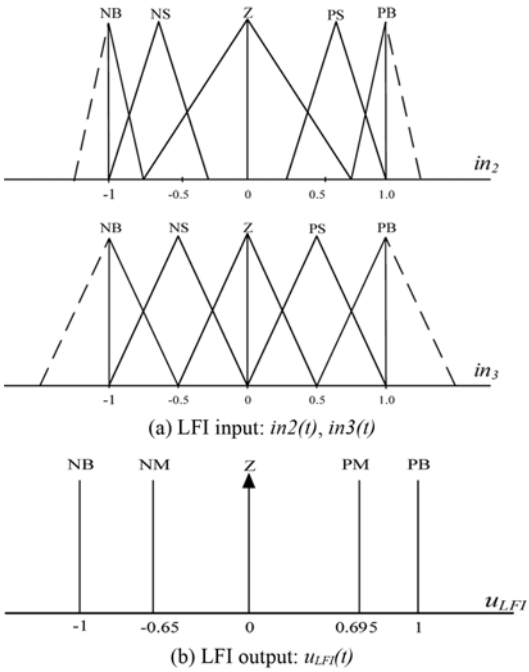

Fig. 9 MFs of the LFI inputs and output

Mechanism' (NLM) to optimize the LFI structure. There are three inputs to the model: the applied current in_1, damper rod displacement in_2 and its velocity in_3. The model output is the estimated damping force, f_{MR_est}, corresponding to these inputs and can be computed as:

$$f_{MR\_est} = u_{LFI} k_{FGI} \tag{1}$$

where: u_{LFI} and k_{GFI} are in turn the output of LFI block and the output of GFI block; The sign of the estimated force depends on the sign of the damper rod velocity.

Here, the GFI inference is designed with fixed structure while the LFI inference is designed based on the Lyapunov criterion and trained by the NLM mechanism. To evaluate the accuracy of the STLFM model, an error function (E) is derived as the difference between the damping force estimated by the model (f_{MR_est}) and the actual damping force (f_{MR}). This error function is defined as the following:

$$E = 0.5(f_{MR\_est} - f_{MR})^2 \tag{2}$$

A. Lyapunov-Based Fuzzy Inference (LFI)

The LFI system takes part in estimating the damping force caused by the applied displacement/velocity to the damper. As seen in Fig. 8, the LFI fuzzy set is therefore designed with two inputs (in_2, in_3) and one output (u_{LFI}). The ranges of these inputs are from -1 to 1, which are obtained from the applied displacement, and its derivative (velocity) through scale factors chosen from the range of displacement and specifications of the MR fluid damper. The fuzzy output range is also set from -1 to 1. From each input variables, five triangle membership functions (MFs) are used and named as "NB" (Negative Big), "NS" (Negative Small), "Z" (Zero), "PS" (Positive Small), and "PB" (Positive Big). The centroids and shapes of these MFs are initially decided as in Fig. 9(a) based on the damper characteristics investigated through the experiments on the test rig (for example, see Fig. 6 and 7). Each MF

of the inputs can be expressed as follow:

$$\mu(x_i) = \frac{1-2|x_i - a_{ji}|}{b_{ji}}, \quad j = 1,2,\ldots,N, \quad i = 1 \text{ or } 2 \tag{3}$$

where a_j is the center of the j^{th} triangle and b_j is width; N is the number of triangles.

For a pair of inputs (in_2, in_3), the LFI output can be computed as:

$$u_{LFI} = \frac{\sum_{k=1}^{M} \mu(w_k) w_k}{\sum_{k=1}^{M} \mu(w_k)} \tag{4}$$

where: w_k and (w_k) are the weights and heights of the LFI output, respectively; M is the number of fuzzy output sets (M=5). The height $\mu(w_k)$ is computed by using the fuzzy output function:

$$\mu(w_k) = \sum_{i,j} \mu_{ij}(w_k) \tag{5}$$

where $\mu_{ij}(wk)$ is defined as the consequent fuzzy output function when the first and second LFI inputs are in the i and j class, respectively:

$$\mu_{ij}(w_k) = \delta_{ij} \mu_{ij} \tag{6}$$

where δ_{ij} is an activating factor which is active when the input in_2 is in class i^{th}, and the input in_3 is in class j^{th}; μ_{ij} is the height of the consequent fuzzy function obtained from the input classes, i^{th} and j^{th}:

$$\mu_{ij} = \min[\mu_i(x_1), \mu_j(x_2)] \equiv \min[\mu_i(in_2), \mu_j(in_3)] \tag{7}$$

where $\mu_i(in_2)$ and $\mu_i(in_3)$ are obtained from (3).

The output u_{LFI} of the LFI system contains five single output values: "NB", "NS", "ZE", "PS", and "PB", within the range from -1 to 1, with the same meaning as the MFs of the inputs. Initial positions of the output weights are decided from the experiments with a constant supplied current where the damping force values were caused by the corresponding points of input displacement and velocity. Fig. 9(b) displays the initial output weight distribution.

As mentioned above, the LFI is designed based on the Lyapunov stability condition which enables to systematically derive the fuzzy rule base. By following the Lyapunov stability condition, a function candidate V is constructed and then, the required conditions to design the LFI system are determined.

Firstly, consider a general system as follows:

$$\begin{cases} \dot{x}(t) = F(x(t), u(t)) \\ y(t) = h(x(t)) \end{cases} \tag{8}$$

where, $x=(x_1, x_2, \ldots, x_n)^T \in \Re^n$ is the input vector of the system, $u \in \Re^m$ is the control input, F: $\Re^{n\times m} \to \Re^n$, $y \in \Re^r$ and h: $\Re^n \to \Re^r$. The control objective is to stabilize the system around some working point x_0 (without loss of generality we assume x_0=0). The Lyapunov function candidate $V(x)$ must satisfy the conditions as follows:

a) $V(0) = 0$ (9)

b) $V(x) > 0, \quad x \in N \setminus \{0\}$ (10)

c) $\dot{V} = \sum_i^n \frac{\partial V}{\partial x_i} \dot{x}_i < 0, \quad x \in N \setminus \{0\}$ (11)

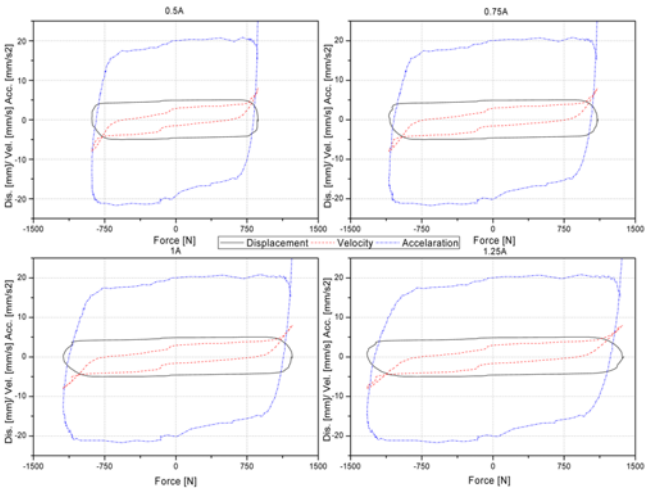

Fig. 10 Experimental results: displacement, velocity and acceleration vs. force at a sinusoidal exc. (2.5Hz and 5mm)

Table 1 Rules table for the LFI of the STLFM model

LFI output u_{LFI}		LFI input 03 - Scaled velocity				
		NB	*NS*	*ZE*	*PS*	*PB*
LFI input 02 - Scaled displacement	*NB*	NB	NB	ZE	PS	PB
	NS	NB	NB	NS	PS	PB
	ZE	NS	NS	ZE	PS	PS
	PS	NB	NS	PS	PB	PB
	PB	NB	NS	ZE	PB	PB

where, $N \setminus \{0\} \in R^n$ is some neighborhood of 0 excluding the origin 0 itself, and $\dot{x}_i$ (i = 1, 2, …) is given by (8).

If x_0 is an equilibrium point of (9) and such V exists, then x_0 is locally asymptotically stable. Let define V=½(x_1^2+x_2^2) as the Lyapunov function candidate. It is clearly that V satisfies (9) and (10). Since $\dot{V} = x_1\dot{x}_1 + x_2\dot{x}_2$ where x_1=x and x_2=$\dot{x}$ then to satisfy (11), it requires that $x\dot{x} + \dot{x}\ddot{x} < 0$ which can be obtained as follow:

$$\dot{V} < 0 \Leftrightarrow \begin{bmatrix} x, \dot{x} > 0, \ddot{x} < -x; \\ x, \dot{x} < 0, \ddot{x} > -x; \\ x > 0, \dot{x} < 0, \ddot{x} > -x; \\ x < 0, \dot{x} > 0, \ddot{x} < -x; \end{bmatrix} \tag{12}$$

Next, the Lyapunov theory is applied to design the rule table of the LFI by considering this model as a controller. Here, the model inputs (the piston displacement and velocity) represent as the system state and, the output (estimated damping force) functions as the control input. By analyzing the relation between the MR damper displacement, velocity, acceleration and damping force, as one experiment shown in Fig. 10, it can be seen that the MR damping behavior with respect to a fixed supply current could satisfy the sufficient robust condition (12). The LFI rules are finally established based on the damping behavior to hold the condition (12) as shown in Table 1. Therefore, the stability of LFI model can be guaranteed.

Furthermore, to optimize the design of the LFI input/output MFs, the decisive factors of the inputs MFs, a_{ji}, b_{ji}, and the output, w_k, are automatically adjusted by computing efficiently partial derivatives of the error function E realized by the model network with respect to all

these decisive elements. The key idea is that these input MFs and the corresponding output weights are only trained if their factors δ_{ij} in (6) are activated. Using this concept for each step, there are maximum 12 LFI factors (8 of the input MFs and 4 corresponding output weights) are updated with respect to the error minimization (in case of maximum 4 rules are activated). A following set of equations shows the back-propagation algorithm based on the gradient descent method for updating the decisive factors at a step of time $(t+1)^{th}$ (see Fig. 8).

$$\left.\begin{aligned} a_{ji}\big|_{t+1} &= a_{ji}\big|_t - \eta_a \frac{\partial E}{\partial a_{ji}}\Big|_t \\ b_{ji}\big|_{t+1} &= b_{ji}\big|_t - \eta_b \frac{\partial E}{\partial b_{ji}}\Big|_t \\ w_k\big|_{t+1} &= w_k\big|_t - \eta_w \frac{\partial E}{\partial w_k}\Big|_t \end{aligned}\right\} \tag{13}$$

where η_a, η_b and η_c are the learning rate which determine the speed of learning; E is the error function defined by (2).

The factor $\partial E/\partial w_{ji}$ in (12) can be calculated as:

$$\frac{\partial E}{\partial w_{ji}} = \frac{\partial E}{\partial f_{MR\_est}} \frac{\partial f_{MR\_est}}{\partial u_{LFI}} \frac{\partial u_{LFI}}{\partial w_i} \tag{14}$$

where:

$$\frac{\partial E}{\partial f_{MR\_est}} = e(t) = f_{MR\_est}(t) - f_{MR}(t) \tag{15}$$

$$\frac{\partial f_{MR\_est}}{\partial u_{LFI}} = k_{GFI} \tag{16}$$

$$\frac{\partial u_{LFI}}{\partial w_i} = \frac{\mu_i}{\Sigma \mu_{ki}} \times k_{GFI} \tag{17}$$

The next factors $\partial E/\partial a_{ji}$ and $\partial E/\partial b_{ji}$ in (13) can be found by:

$$\frac{\partial E}{\partial a_i} = \frac{\partial E}{\partial f_{MR\_est}} \frac{\partial f_{MR\_est}}{\partial u_{LFI}} \frac{\partial u_{LFI}}{\partial \mu_i} \frac{\partial \mu_i}{\partial a_i} \tag{18}$$

$$\frac{\partial E}{\partial b_{ji}} = \frac{\partial E}{\partial f_{MR\_est}} \frac{\partial f_{MR\_est}}{\partial u_{LFI}} \frac{\partial u_{LFI}}{\partial \mu_i} \frac{\partial \mu_i}{\partial b_i} \tag{19}$$

where,

$$\frac{\partial u_{LFI}}{\partial \mu_i} = \frac{\sum_{k=1}^{M} \mu_k (w_i - w_k)}{\left(\sum_{k=1}^{M} \mu_k\right)^2} \times k \tag{20}$$

$$\frac{\partial \mu_i}{\partial a_i} = sign(x - a_i) \frac{2}{b_i} \tag{21}$$

$$\frac{\partial \mu_i}{\partial b_i} = \frac{2|x - a_i|}{b_i^2} \tag{22}$$

$\partial E/\partial f_{MR\_est}$, $\partial f_{MR\_est}/\partial u_{LFI}$ is calculated by using (15) and (16), respectively.

B. Gain Fuzzy Inference (GFI)

This section presents the description of the gain fuzzy inference which is used as a switch to turn the damping force with levels with respect to the current supplied for the MR damper. The GFI system is designed with a single input in_1 and a single output k_{GFI} (see Fig. 8). The range of the input is from 0 to 1, which is obtained from the supplied current through a scale factor chosen from the current range

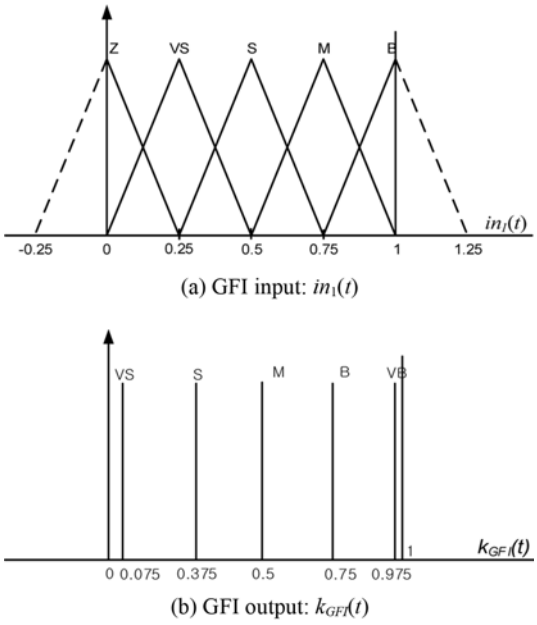

Fig. 11 MFs of the GFI inputs and output

Table 2 Rules table for the GFI of the STLFM model

GFI input - Scaled supplied current (in_1)	Z	VS	S	M	B
GFI output (k_{GFI})	VS	S	M	B	VB

for the MR fluid damper coil. Five triangle MFs, "Z" (Zero), "VS" (Very Small), "S" (Small), "M" (Medium), and "B" (Big), were used for this input variable. These MFs and their centroids were initially set with a same shape and at same intervals, respectively, in Fig. 11(a).

By using the same fuzzy design method as that of the LFI system to design the GFI, the output gain (k_{GFI}) corresponding to an input value (in_1) can be calculated as

$$k_{GFI} = \frac{\sum_{q=1}^{R} w_q \mu(w_q)}{\sum_{q=1}^{R} \mu(w_q)} \tag{23}$$

where: w_q and $\mu(w_q)$ are the weight and its height of the GFI output, respectively. R is the number of fuzzy output sets (R=5). For the output k_{GFI} of the GFI system, five MFs were used and named as "VS" (Very Small), "S" (Small), "M" (Medium), "B" (Big), and "VB" (Very Big). The output range is set from 0 to 1. The estimated damping force level is then obtained by multiplying the GFI output and a suitable scale factor. By using the above fuzzy sets of the input and output variables, the fuzzy rules for the GFI are established in Table 2 by using the IF-THEN structure.

Finally, the output of the estimation force can be computed from the LFI output (u_{LFI}) and GFI output (k_{GFI}) using (1).

3. Modeling Results

In order to derive the STLFM model with high accuracy, real-time experiments with opened-loop control on the damper test rig were firstly

performed to obtain the actual damping behavior. Next based on a training data select from the experiments, the model training process was carried out to find out the STLFM with optimized parameters. Finally, simulations with the optimized STLFM were performed to evaluate the ability of this model when comparing with the actual dynamic responses of the damper. All the programs for data observation as well as for constructing the model were built in the Simulink environment combined with Real-Time Windows Target toolbox of MATLAB with 0.01s of sampling period.

3.1 Model optimization

The optimization process as mentioned in Section 2.3 A was then carried out for the model training purpose. A set of experimental data of the damper corresponding to an excitation of the damper rod with 2.5 Hz of frequency and 5 mm of amplitude (Fig. 12(a)) while the current supplied for the damper coil was 0.75 A was used as the model training data.

In order to evaluate how well the model fits with the actual MR damper, the goodness of fit [%] was calculated using the normalize root mean square error:

$$fit = 1 - \frac{\|\hat{Y} - Y\|}{\|Y - mean(Y)\|} \tag{24}$$

here: Y and $\hat{Y}$ are the training data vector and the corresponding model output vector.

After training, the LFI parameters of the STLFM optimized by the leaning mechanism with respect to the modeling error cost function were displayed in Fig. 13. As a result, the modeling results were then obtained as drawn in figures from 12(b) to 12(d). The results show that with the model designed in Section 2, the nonlinear characteristic of the damper could be directly estimated with high accuracy for both the force/time, force/displacement, and force/velocity relations. The goodness of fit of the model with optimized parameters was 95.67%.

3.2 Model verification

In this section, the STLFM optimized in Section 3.1 has been validated through series of experiments and simulations. Firstly, the comparison between the actual and simulated MR damper performances was done with respect to the same excitation of the damper rod as drawn in Fig. 12(a) while the current supplied for the damper coil was varied from 0 to 1.5A.The comparison results as displayed in Fig. 14 point out that the optimized model could represent well the damping behavior when the supply current varied.

Next, the modeling with different excitation signals and supply currents were carried out to evaluate the model capability. Furthermore, a comparison of the damping force estimation results between a Bingham model, a Bouc-Wen model and the proposed model was also performed to assess clearly the modelling efficiency.

3.2.1 Bingham model

The stress-strain behavior of the Bingham visco-plastic model is often used to describe the behavior of MR fluid. Based on this model, an idealized mechanical model referred to as the Bingham model was proposed to estimate the behavior of an MR fluid damper by Standway et al.[15] Here, for nonzero piston velocities, $\dot{x}$, the force F generated by the device is given by:

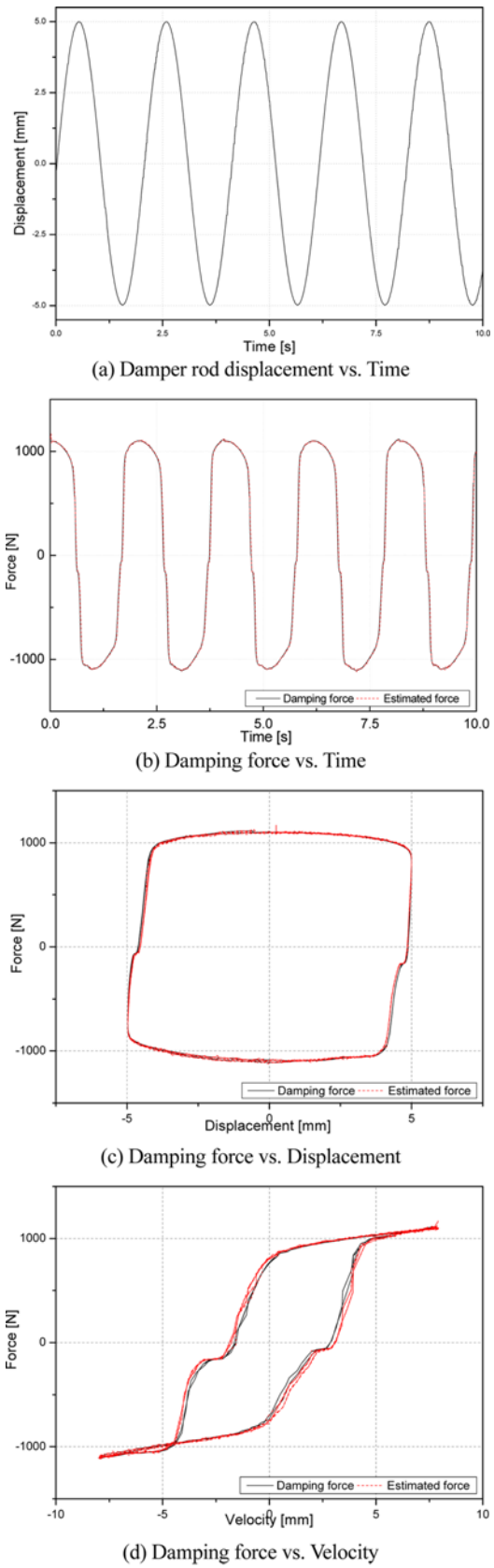

(a) Damper rod displacement vs. Time

(b) Damping force vs. Time

(c) Damping force vs. Displacement

(d) Damping force vs. Velocity

Fig. 12 Model training results corresponding to a sinusoidal excitation (2.5 Hz, 5 mm) and 0.75 A of supply current

$$F_{Bingham} = f_c \text{sign}(\dot{x}) + c_0 \dot{x} + f_0 \tag{25}$$

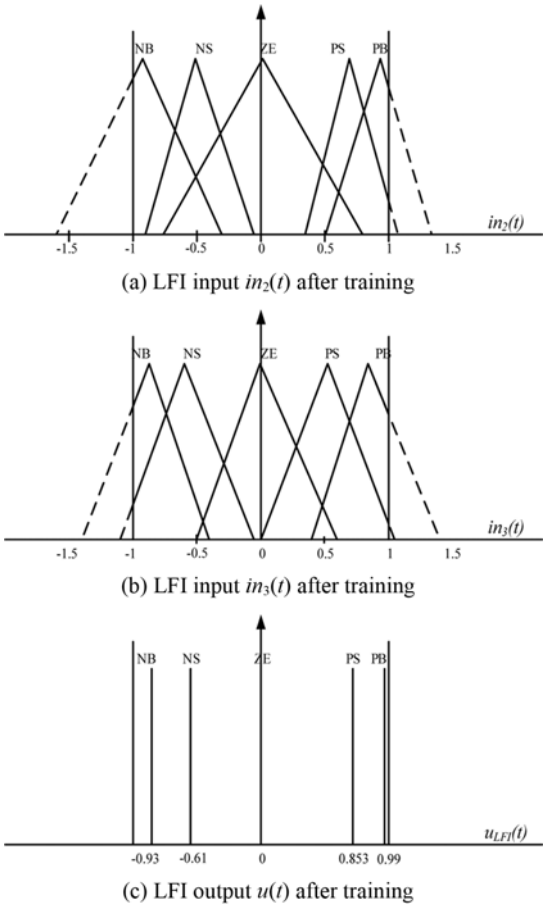

Fig. 13 MFs of the LFI inputs and output after training

where c_0 is the damping coefficient; f_c is the frictional force related to the fluid yield stress; and an offset in the force f_0 is included to account for the nonzero mean observed in the measured force due to the presence of the accumulator.

To present the damper behavior, the characteristic parameters of the Bingham model in Eq. (25) need to be chosen to fit with the experimental data of the damping system. For example, those parameters were chosen as c_0=50 Ns/cm; f_c=950 N and f_0=75 N.

3.2.2 Bouc-Wen model

Here, the Bouc-Wen model was developed and optimized by Kwok et al.[19] This model can be described by the force equation and the associated hysteretic variable as given:

$$\begin{aligned} F_{Bouc\text{-}Wen} &= c\dot{x}+kx+az+f_0 \\ \dot{z} &= -\gamma|\dot{x}||z|z|^{n-1}-\beta\dot{x}|z|^n+\delta\dot{x} \end{aligned} \tag{26}$$

where: F is the damping force; f_0 is the offset force; c is the viscous coefficient; k is the stiffness, $\dot{x}$ and x are the damper velocity and displacement; α is a scaling factor; z is the hysteretic variable; and γ, β, δ, n are the model parameters to be identified. Note that when α=0, the model represents a conventional damper.

As the optimization results for the damping system using the same damper RD-1005-3 by using GA in Ref. 19, the relationships between the Bouc-Wen parameters and the supplied magnetization current, i, were given as:

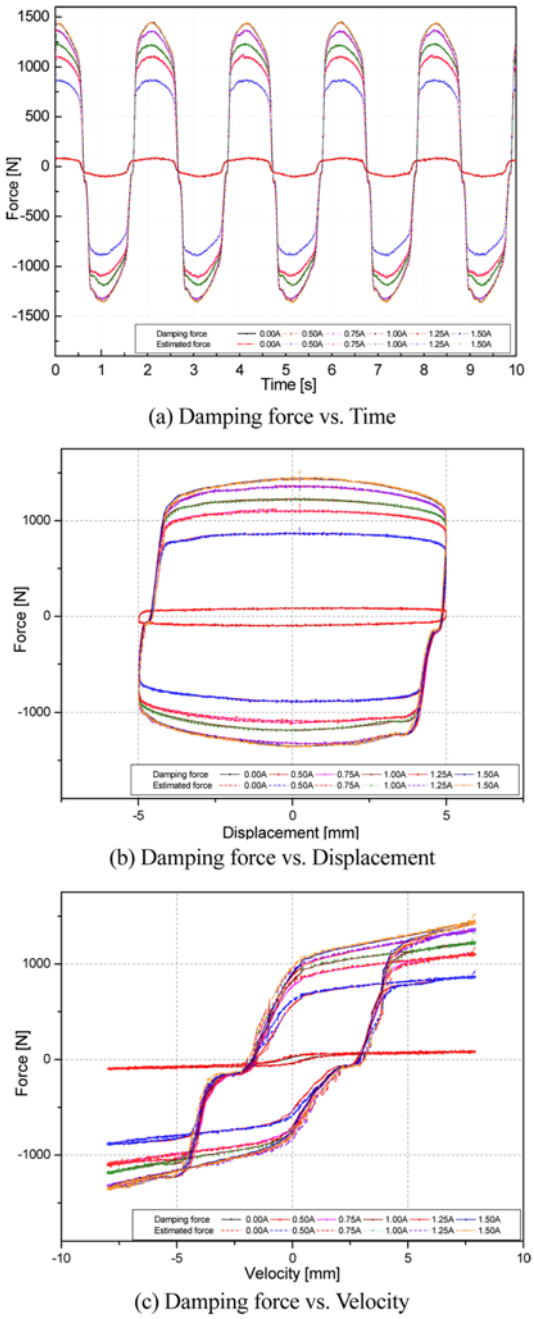

Fig. 14 Model verification results corresponding to a sinusoidal excitation (2.5 Hz, 5 mm) and a range of supply current [0.5, 1.5] A

$$\begin{aligned} c &= 2.65\times10^3 i+2.05\times10^3; \quad k = 1.99\times10^3 i+5.57\times10^3; \\ \alpha &= 2.11\times10^3 i+1.68\times10^3; \quad f_0 = 0.6i-12.43; \\ \mu &= -0.02i+1.25; \quad n = 0.12i+1.58; \quad \gamma = 0.39\times10^6 i+3.6\times10^6 \\ \delta &= 0.5\times10^5 i+2.5\times10^5; \quad \beta = -0.45\times10^6 i+3.18\times10^6; \end{aligned} \tag{27}$$

3.3.3 Comparison results

The simulations using the compared models were then conducted with a 2.5 Hz sinusoidal excitation with amplitude 5 mm while the supply current was 0.5 A. The comparison between the actual damping performance and the modeling performances is shown in Fig. 15. The results indicate that the modeling results using the Bingham model (the

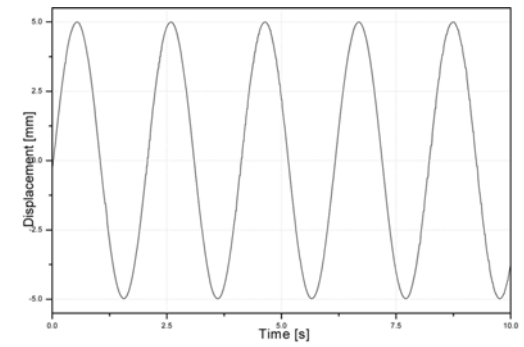

(a) Damper rod displacement vs. Time

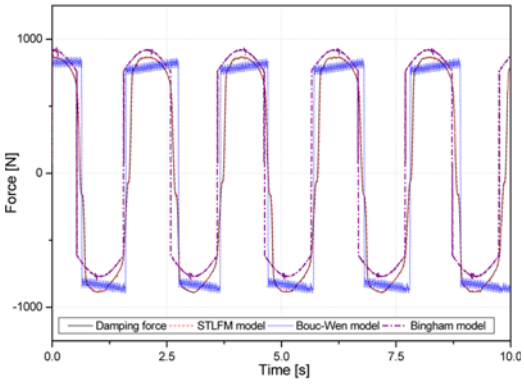

(b) Damping force vs. Time

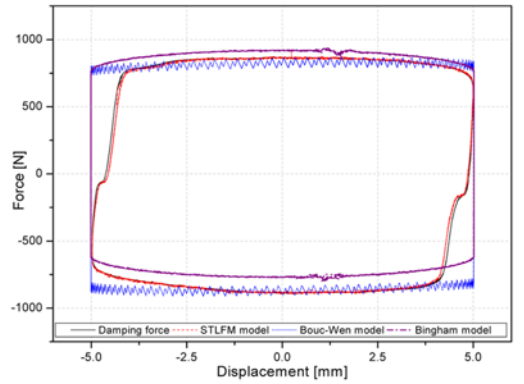

(c) Damping force vs. Displacement

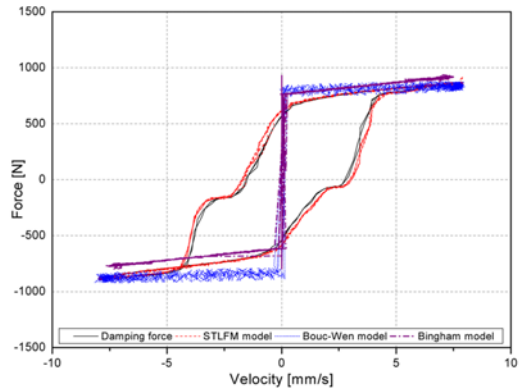

(d) Damping force vs. Velocity

Fig. 15 Modeling performances using different models corresponding to a sinusoidal excitation (2.5 Hz, 5 mm) and 0.5 A of supply current

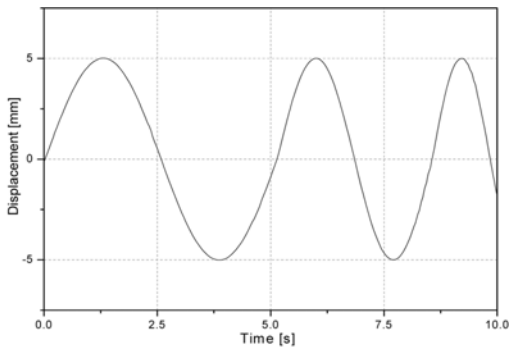

(a) Damper rod displacement vs. Time

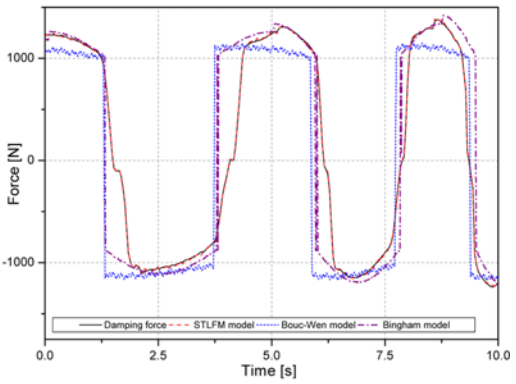

(b) Damping force vs. Time

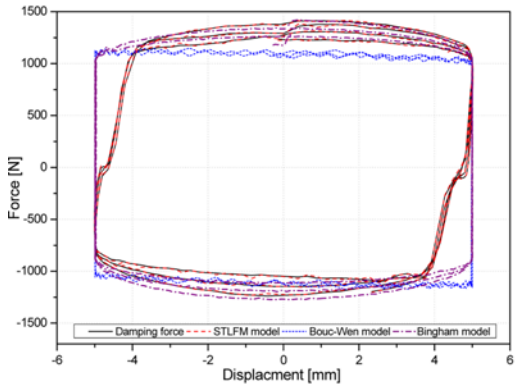

(c) Damping force vs. Displacement

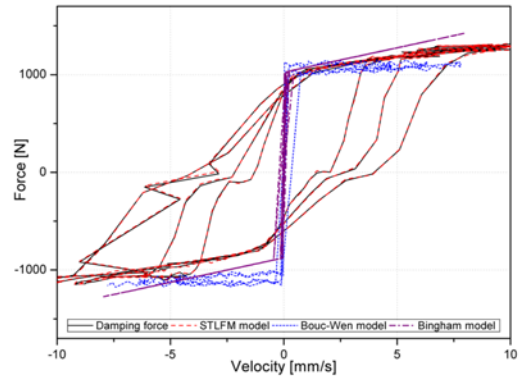

(d) Damping force vs. Velocity

Fig. 16 Modeling performances using different models corresponding to a chirp excitation ([0.2, 1] Hz, 5mm) and 1A of supply current

dash-dot purple lines) were not acceptable, especially for velocity that were near zero. By using this model the relationship between the force and velocity was one-to-one, but the experimentally obtained data was not one-to-one. The performance of the Bouc-Wen model (the short-

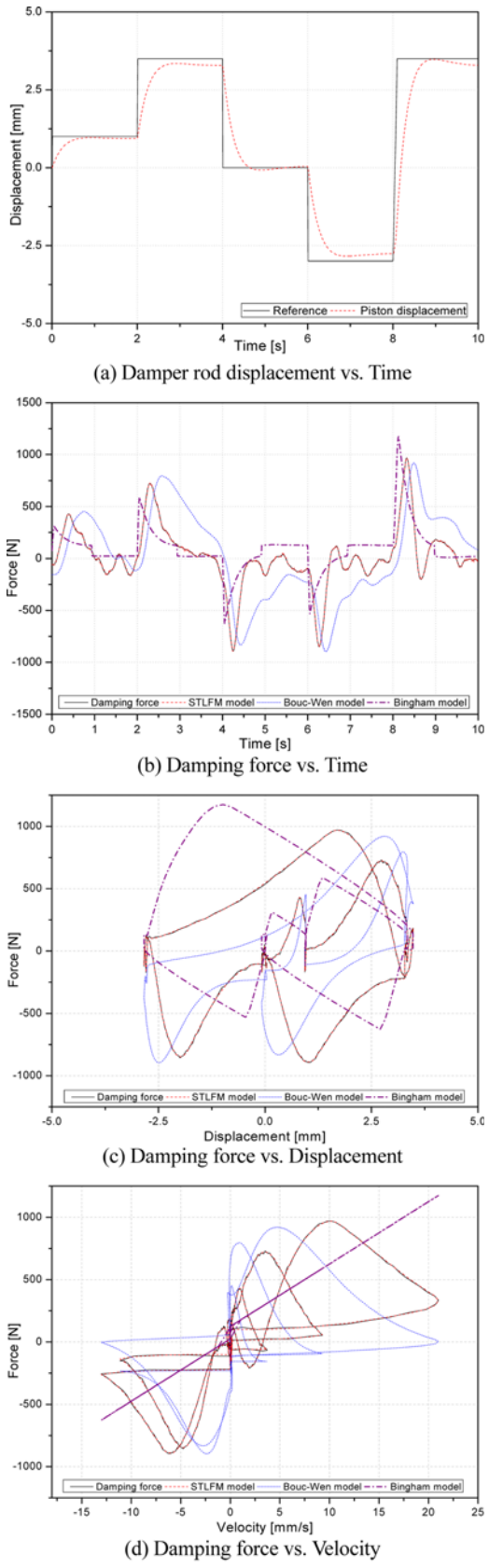

Fig. 17 Modeling performances using different models corresponding to a multi-step excitation and 0.75A of supply current

dash blue lines) was also different from the actual performance. The reasons was that its parameter were though optimized in the previous study,[19] it is necessary to optimize again when applied to another system using the same damper. Meanwhile, the optimized STLFM model could estimate the damping characteristic with acceptable performance (the dash red lines). The goodness of fit of the model with optimized parameters was 94.35%.

Finally, the models were validated with a chirp excitation and a multi-step excitation of the damper rod while the supply currents were in turn 1 A and 0.75 A. Here, the chirp signal was with the frequency range [0.2, 1 Hz] and 5 mm of the amplitude (Fig. 16(a)) while the multi-step signal was described in Fig. 17(a). Subsequently, the modeling results were obtained and plotted in Figs. 16 and 17, respectively. These results show that the Bouc-Wen model and Bingham model could not enhance the desired modeling performance, especially in representing the force-displacement and force-velocity relations. On the contrary with different working conditions, excitations and supply currents, the STLFM with optimized parameters always brought to the good modeling performances of the MR damper with small errors in most regions when compared with the actual performances. It is clearly visible that the proposed model could predict fairly well the hysteresis behavior under various conditions.

4. Conclusions

This paper developed the self-tuning Lyapunov-based fuzzy model for MR fluid damper to estimate directly the damping characteristics with high precision. The simple test rig using the researched damper was setup for the investigation. Firstly, the model was constructed in the form of a center average fuzzy interference system, of which the fuzzy rules were designed based on the Lyapunov stability condition. Secondly in order to optimize the STLFM, the training process based on the back propagation learning rules and the practical damping data obtained from the experimental system was used to adjust the fuzzy parameters. Finally, the optimized model was evaluated with the Bouc-Wen and the Bingham models in predicting the damping characteristics with respect to the different excitations and supply current levels. The comparison results prove convincingly that the developed model could achieve the better performances over the other models. By using the STLFM, the modeling results were almost fit to the actual damping data with acceptable errors in both force-time, force-displacement and force-velocity relations, especially in low supply current levels. The STLFM model can be an effective tool for engineers and researchers to further exploit benefits of MR fluid dampers in semi-active control.

ACKNOWLEDGEMENT

This work was supported by 2014 Special Research Fund of Mechanical Engineering at the University of Ulsan.

REFERENCES

1. Di Monaco, F., Ghandchi Tehrani, M., Elliott, S. J., Bonisoli, E., and Tornincasa, S., “Energy Harvesting using Semi-Active Control,”

Journal of Sound and Vibration, Vol. 332, No. 23, pp. 6033-6043, 2013.

2. Turnip, A., Park, S., and Hong, K. S., "Sensitivity Control of a MR-Damper Semi-Active Suspension," Int. J. Precis. Eng. Manuf., Vol. 11, No. 2, pp. 209-218, 2010.
3. Lee, G. M., Ju, Y. H., and Park, M. S., "Development of a Low Frequency Shaker using MR Dampers," Int. J. Precis. Eng. Manuf., Vol. 14, No. 9, pp. 1647-1650, 2013.
4. Bitaraf, M. and Hurlebaus, S., "Semi-Active Adaptive Control of Seismically Excited 20-Story Nonlinear Building," Engineering Structures, Vol. 56, No. pp. 2107-2118, 2013.
5. Weber, F., "Semi-Active Vibration Absorber based on Real-Time Controlled MR Damper," Mechanical Systems and Signal Processing, Vol. 46, No. 2, pp. 272-288, 2014.
6. Lee, H. G., Sung, K. G., Choi, S. B., Park, M. K., and Park, M. K., "Performance Evaluation of a Quarter-Vehicle MR Suspension System with Different Tire Pressure," Int. J. Precis. Eng. Manuf., Vol. 12, No. 2, pp. 203-210, 2011.
7. Kim, H. J., "Passive and Semi-Active Shock Reduction for Prototype HSRMD Avoiding Human Damage," Int. J. Precis. Eng. Manuf., Vol. 12, No. 2, pp. 219-225, 2011.
8. Ahmed, G. M. S., Reddy, P. R., and Seetharamaiah, N., "Experimental Investigation of Magneto Rheological Damping Effect on Surface Roughness of Work Piece during End Milling Process," Int. J. Precis. Eng. Manuf., Vol. 13, No. 6, pp. 835-844, 2012.
9. Yi, K. and Song, B., "A New Adaptive Sky-Hook Control of Vehicle Semi-Active Suspensions," Proceedings of the Institution of Mechanical Engineers, Part D: Journal of Automobile Engineering, Vol. 213, No. 3, pp. 293-303, 1999.
10. Mizuno, T., Kobori, T., Hirai, J. I., Matsunaga, Y., and Niwa, N., "Development of Adjustable Hydraulic Dampers for Seismic Response Control of Large Structure," Proc. of ASME PVP Conference, pp. 163-170, 1992.
11. Kwok, N. M., Ha, Q. P., Nguyen, T. H., Li, J., and Samali, B., "A Novel Hysteretic Model for Magnetorheological Fluid Dampers and Parameter Identification using Particle Swarm Optimization," Sensors and Actuators A: Physical, Vol. 132, No. 2, pp. 441-451, 2006.
12. Choi, S. B., Lee, S. K., and Park, Y. P., "A Hysteresis Model for the Field-Dependent Damping Force of a Magnetorheological Damper," Journal of Sound and Vibration, Vol. 245, No. 2, pp. 375-383, 2001.
13. Vadtala, I. H., Soni, D. P., and Panchal, D. G., "Semi-Active Control of a Benchmark Building using Neuro-Inverse Dynamics of MR Damper," Procedia Engineering, Vol. 51, pp. 45-54, 2013.
14. Wang, D. H. and Liao, W. H., "Modeling and Control of Magnetorheological Fluid Dampers using Neural Networks," Smart Materials and Structures, Vol. 14, No. 1, pp. 111, 2005.
15. Stanway, R., Sproston, J., and Stevens, N., "Non-Linear Modelling of an Electro-Rheological Vibration Damper," Journal of Electrostatics, Vol. 20, No. 2, pp. 167-184, 1987.
16. Dominguez, A., Sedaghati, R., and Stiharu, I., "Modelling the Hysteresis Phenomenon of Magnetorheological Dampers," Smart Materials and Structures, Vol. 13, No. 6, pp. 1351, 2004.
17. Bouc, R., "Forced Vibration of Mechanical Systems with Hysteresis," Proc. of the 4th Conference on Non-Linear Oscillation, p. 315, 1967.
18. Wen, Y. K., "Method for Random Vibration of Hysteretic Systems," Journal of the Engineering Mechanics Division, Vol. 102, No. 2, pp. 249-263, 1976.
19. Kwok, N. M., Ha, Q. P., Nguyen, M. T., Li, J., and Samali, B., "Bouc-Wen Model Parameter Identification for a MR Fluid Damper using Computationally Efficient GA," ISA transactions, Vol. 46, No. 2, pp. 167-179, 2007.
20. Çemeci, S. and Engin, T., "Modeling and Testing of a Field-Controllable Magnetorheological Fluid Damper," International Journal of Mechanical Sciences, Vol. 52, No. 8, pp. 1036-1046, 2010.
21. Peng, G. R., Li, W. H., Du, H., Deng, H. X., and Alici, G., "Modelling and Identifying the Parameters of a Magneto-Rheological Damper with a Force-Lag Phenomenon," Applied Mathematical Modelling, Vol. 38, No. 15-16, pp. 3763-3773, 2014.
22. Spencer, B. F., Dyke, S. J., Sain, M. K., and Carlson, J. D., "Phenomenological Model of a Magneto-Rheological Damper," Journal of Engineering Mechanics, Vol. 123, No. 3, pp. 230-238, 1996.
23. Chang, C. C. and Roschke, P., "Neural Network Modeling of a Magnetorheological Damper," Journal of Intelligent Material Systems and Structures, Vol. 9, No. 9, pp. 755-764, 1998.
24. Schurter, K. C. and Roschke, P. N., "Fuzzy Modeling of a Magnetorheological Damper using Anfis," Prof. of the 9th IEEE International Conference on Fuzzy Systems, Vol. 1, pp. 122-127, 2000.
25. Wang, D. H. and Liao, W. H., "Neural Network Modeling and Controllers for Magnetorheological Fluid Dampers," Proc. of the 10th IEEE International Conference on Fuzzy Systems, Vol. 3, pp. 1323-1326, 2001.
26. Margaliot, M. and Langholz, G., "Fuzzy Lyapunov-based Approach to the Design of Fuzzy Controllers," Fuzzy Sets and Systems, Vol. 106, No. 1, pp. 49-59, 1999.
27. Roy, A. and Sharma, K. D., "Gravitational Search Algorithm and Lyapunov Theory based Stable Adaptive Fuzzy Logic Controller," Procedia Technology, Vol. 10, pp. 581-586, 2013.
28. Margaliot, M. and Langholz, G., "Design and Analysis of Fuzzy Schedulers using Fuzzy Lyapunov Synthesis," Engineering Applications of Artificial Intelligence, Vol. 14, No. 2, pp. 183-188, 2001.